ACS APPLIED MATERIALS & INTERFACES

Research Article

www.acsami.org

Facile Preparation of Lightweight Microcellular Polyetherimide/Graphene Composite Foams for Electromagnetic Interference Shielding

Jianqiang Ling,[†,‡] Wentao Zhai,[*,†] Weiwei Feng,[†] Bin Shen,[†] Jianfeng Zhang,[‡] and Wen ge Zheng[†]

[†]Ningbo Key Lab of Polymer Materials, Ningbo Institute of Material Technology and Engineering, Chinese Academy of Sciences, Ningbo, Zhejiang Province, 315201, China

[‡]The School of Materials Science and Chemical Engineering, Ningbo University, Ningbo, Zhejiang Province, 315211, China

ABSTRACT: We report a facile approach to produce lightweight microcellular polyetherimide (PEI)/graphene nanocomposite foams with a density of about 0.3 g/cm^3 by a phase separation process. It was observed that the strong extensional flow generated during cell growth induced the enrichment and orientation of graphene on cell walls. This action decreased the electrical conductivity percolation from 0.21 vol % for PEI/graphene nanocomposite to 0.18 vol % for PEI/graphene foam. Furthermore, the foaming process significantly increased the specific electromagnetic interference (EMI) shielding effectiveness from 17 to 44 dB/(g/cm^3). In addition, PEI/graphene nanocomposite foams possessed low thermal conductivity of 0.065−0.037 W/m·K even at 200 °C and high Young's modulus of 180−290 MPa.

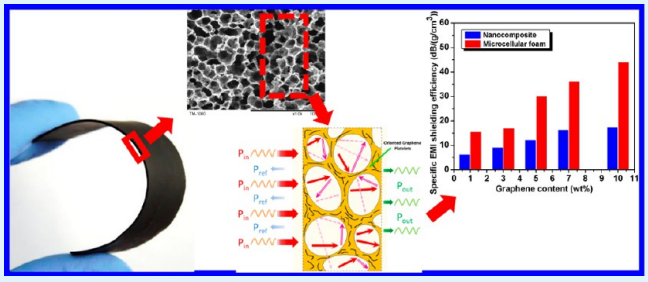

KEYWORDS: *polyetherimide, microcellular foam, graphene, electrical conductivity, electromagnetic interference shielding*

1. INTRODUCTION

Because of the wide use of commercial, military, and scientific electronic devices and communication instruments, electromagnetic interference (EMI) shielding of radio frequency radiation continues to be a serious concern for modern society. The preparation of EMI shielding materials has obtained an increased attention in the academic and industrial fields. Compared to the conventional metal-based EMI materials, polymer composites containing carbon-based nanofillers have their own advantages, such as being lightweight, resistance to corrosion, excellent processability, and broad absorption bandwidth.[1−3] Graphene, a new class of 2D carbon nanomaterial, possesses extraordinary electrical, mechanical, and thermal properties.[4] These unique features offer great promise for its use in EMI shielding.[5−7] Besides, for the application in special fields such as aerospace, weapon equipment, vehicles, and microelectronics where the materials with superior thermal stability, excellent mechanical properties, perfect radiation, and electrical resistant performance are required, high performance polymer instead of general polymer could be a better candidate to fulfill the task.

Being lightweight is a key technological requirement for the development of practical EMI shielding material.[8] A novel approach to achieve this purpose is to produce polymeric foams.[6−11] Yang et al. prepared polystyrene (PS)/carbon nanofiller composite foams using a chemical blowing agent. They found that the EMI shielding effectiveness (SE) of the as-produced composite foams were 14 dB for 10 wt % nanofiber loading and 19 dB for 15 wt % nanofiber loading, respectively.[8,9] Furthermore, Zhang et al. fabricated PMMA/graphene foams using supercritical CO_2 as a physical blowing agent, and the prepared composite foams with 5 wt % graphene loading exhibited an EMI SE of 13−19 dB.[6] Besides PS and PMMA, other polymer systems such as polyurethane (PU)[12] and polycaprolactone (PCL)[13] have also been used for the fabrication of EMI shielding materials. However, the general properties of these polymers, such as low heat-resistance, poor flame retardancy, and high smoke generation, restrict their use as the EMI shielding materials in aerospace and other special fields.

Polyetherimide (PEI) is a kind of high-performance polymer, which possesses a high T_g of 215 °C, excellent flame retardancy, low smoke generation, and good mechanical properties. The preparation of PEI composite foams for EMI shielding is very meaningful for high-tech applications. Unfortunately, several technical challenges are present in preparation of lightweight PEI composite foams, especially at high filler loading. First, the melt compounding is a preferred way to prepare polymer/nanofiller composite. The processing temperature of PEI is as high as 340−360 °C. The introduction of a large amount of fillers tends to significantly increase the viscosity of polymer melt, which make the compounding process very challenging. In the case of polymer nanocomposite with high filler loading, the filling process is very difficult and the nanofillers are easy to

Received: January 11, 2013
Accepted: March 6, 2013
Published: March 6, 2013

aggregate due to the extremely high specific surface area of nanofillers. Second, when the blowing agent such as CO_2 is used to foam PEI, researchers found that an extremely long saturation time,[14] i.e., 280−520 h,[15,16] was required for sheets with thickness of 1.5 mm. This causes a time-consuming process in the preparation of PEI microcellular foam with a large sample size. Finally, after gas saturation, a heating or pressure quenching process is carried out to foam the composites. Unfortunately, polymer composite foam with high filler loading usually exhibits low expansion ratio, usually lower than 2 times in volume expansion,[17] resulting from the high polymer matrix stiffness and the increased gas escape rate.

In this study, we report a facile and fast approach to produce lightweight microcellular PEI/graphene foams for the use of EMI shielding. A water vapor induced phase separation (WVIPS) process was applied to prepare the microcellular PEI/graphene composite foams, and graphene with loading up to 10 wt % was added. Herein, the enrichment and orientation of graphene during the foam processing was emphasized, and the influences of enrichment and orientation of graphene on the electrical conductivity and the EMI shielding effectiveness were explored. The mechanical properties and thermal conductivity of PEI/graphene nanocomposite foams were also discussed. To the best of our knowledge, few studies have declared the preparation of lightweight microcellular high-performance polymer nanocomposite foams for the application in electrical conducting and EMI shielding. This study provided a novel and facile approach to produce high performance, lightweight, and multifunctional polymeric material.

2. EXPERIMENTAL SECTION

2.1. Materials. PEI resin (Ultem1000) was purchased from General Electrical Company, which is a transparent and amber colored particle with a density of 1.28 g/cm^3 and T_g of 215 °C. Pristine graphene was prepared according to the method described in our previous work.[6] The specific surface area of the graphene was 700 m^2/g, measured with a BET method using nitrogen adsorption analysis. The specific surface area is about ∼3.5 times lower than the ideal specific surface area (2630 m^2/g) of a single graphene sheet,[18] which indicated that each graphene platelet was composed of ∼3−4 individual graphene sheets. *N*,*N*′-Dimethyl formamide (DMF) was supplied by Sinopharm Chemical Reagent (China) and was used as received.

2.2. Fabrication of PEI/Graphene Nanocomposites. PEI/graphene nanocomposites were prepared by solution blending. Graphene was first dispersed in DMF at room temperature with the aid of ultrasonication for 30 min. Then, a quantity of PEI particles was dissolved into the graphene suspension with vigorous stirring for 24 h at 70 °C. After that, the resultant solution was added in excessive ethanol, and the produced precipitate was filtrated and dried at 80 °C for 48 h in order to remove the residual ethanol. Finally, a high speed disintegrator was applied to pulverize the dried precipitate into powder for further experiment. The specimens used for electrical conductivity and EMI shielding efficiency measurements were prepared by hot-press at 330 °C.

2.3. Preparation of Microcellular PEI/Graphene Nanocomposite Foams. A WVIPS process was carried out to prepare microcellular PEI/graphene nanocomposite foams. The as-prepared PEI/graphene nanocomposite powder was redissolved in DMF and stirred by a mechanical agitator at a speed of 400 rpm/min for 24 h at 70 °C. The dispersion was poured on a clean glass plate and exposed in the air with a controlled humidity of 75% and temperature of 22 °C. The obtained foam sheets were then immersed in cold water to remove the residual DMF and then dried at 180 °C for 36 h to remove the residual water and DMF.

2.4. Characterizations. The densities of PI/graphene nanocomposites (ρ) and microcellular foams (ρ_f) were measured via the water displacement method in accord with ASTM D792. The morphology of the foamed samples was observed with a Hitachi TM-1000 scanning electron microscope (SEM). The samples were freeze-fractured in liquid nitrogen and sputter-coated with gold. The dispersion and distribution of graphene in the PEI matrix were studied with a Tecnai G2 F20 transmission electron microscopy (TEM) at an accelerating voltage of 100 kV. Before the TEM observation, the samples were embedded in the epoxy resin and then cut into ultrathin slices with thickness of 100 nm.

The volume electrical conductivity of the moderately conductive samples (>1 × 10^{-8} S/cm) was measured using Solartron 1287 electrochemical workstation (Advanced Measurement Technology Inc. USA) with the DC measurement model. The samples with rather low conductivity (≤1 × 10^{-8} S/cm) were measured with three-terminal fixture on an EST121 ultrahigh resistance and microcurrent meter (Beijing EST Science & Technology CO. Ltd.) according to ASTM D257. Circular plates with diameter of 7 cm were prepared for conductivity measurement. The sample surfaces were sputter coated with copper to reduce the contact resistance between the electrodes and the sample. At least five samples were repeated for each test, and the average value was used as the final result.

The EMI shielding property was measured using a WILTRON 54169A scalar measurement system in the frequency range of 8−12 GHz at room temperature. The samples were cut into rectangle plates with a dimension of 22.5 × 10.0 mm^2 to fit the waveguide sample holder. The thickness of samples were about 2.3 mm. The EMI shielding efficiency (SE_{total}) is defined as the logarithmic ratio of incoming (P_i) to outgoing power (P_o) of radiation, and the unit is expressed in decibels (dB). It is the sum of the reflection from the material surface (SE_R), the absorption of electromagnetic energy (SE_A), and the multiple internal reflections (SE_M) of electromagnetic radiation.

The thermal conductivity analysis system (NETZSCH LFA 457 MicroFlash) was used to determine the thermal conductivity of PEI/graphene nanocomposite foams. At least five samples were repeated for each test, and the average value was used as the final result.

ASTM D882-09 was applied to characterize the mechanical properties (Instron 5567) of PEI/graphene nanocomposite foams. The typical dimensions of the specimens were 100 mm × 10 mm × 1 mm. The crosshead speed of the tensile test was 5 mm/min. For each specimen, five samples were tested to obtain the average data of the Young's modulus and tensile strength at break.

3. RESULT AND DISCUSSION

3.1. Fabrication of Microcellular PEI/Graphene Foams. A WVIPS process was used to fabricate PEI/graphene nanocomposite foams. As described in Figure 1, a homogeneous PEI/graphene nanocomposite dispersion was obtained with the help of ultrasonic irradiation and vigorous stirring. After being exposed to air, the cell nucleation took place in PEI/graphene dispersion, which was associated with the occurrence of phase separation, resulting from the diffusion of DMF into dispersion and the diffusion of water vapor into air. As the phase separation continued, the nuclei grew up with the entry of solvent and more importantly with the coalescence of bubbles between each other.[19,20] After removing the solvent in cells, the PEI/graphene nanocomposite foams were obtained.

Table 1 shows the density of PEI/graphene nanocomposite foams as a function of graphene content. The density of PEI foam was 0.28 g/cm^3. It is interesting to find that the introduction of graphene with loading up to 10 wt % did not change the density of PEI/graphene nanocomposite foams. In the case of polymer nanocomposite foams blown with physical blowing agent (PBA), however, researchers found that the addition of 9 wt % nanosilica increased the foam density from

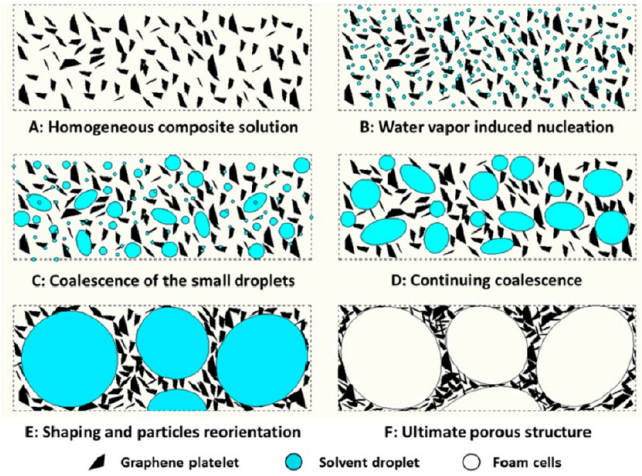

Figure 1. Schematic of WVIPS process to prepare PEI/graphene nanocomposite foam.

Table 1. Density of PEI/Graphene Nanocomposite Foams as the Function of Graphene Content

graphene content in nanocomposite (wt %)	graphene content in nanocomposite (vol %)	graphene content in foams (vol %)	foam density (g/cm^3)
0	0	0	0.28
0.1	0.06	0.01	0.29
0.3	0.17	0.04	0.28
0.5	0.28	0.06	0.28
0.7	0.39	0.09	0.28
1	0.56	0.12	0.28
2	1.13	0.25	0.28
3	1.71	0.39	0.29
5	2.87	0.75	0.32
7	4.05	1.01	0.31
10	5.87	1.38	0.29

0.75 g/cm^3 for pure polycarbonate (PC) foam to 0.92 g/cm^3 for PC nanocomposite foam, due to the increased polymer matrix stiffness.[17] Therefore, compared with the microcellular foaming technology using PBA, the WVIPS process exhibited an obvious advantage in preparing lightweight polymer nanocomposite microcellular foam.

A typical optical micrograph of PEI/graphene nanocomposite foam with graphene loading of 5 wt % is indicated in Figure 2. The thickness of foam sheet was 1.8 mm, and it was quite flexible under bending. Figure 2 shows the cell morphology of PEI/graphene nanocomposite foams, and Table 2 summarizes their average cell diameter. PEI foam possessed microcellular cell structure with cell size of 15.3 μm and uniform cell size distribution. The addition of graphene increased the cell size slightly to 16.3 μm for microcellular foam with graphene loading of 0.5 wt % and to 16.6 μm for microcellular foam with graphene loading of 1 wt %. With a further increase in graphene loading, however, the cell size of PEI/graphene nanocomposites foam tended to decrease to 13.5, 12.1, and 9.0 μm for graphene loading of 5, 7, and 10%, respectively, possibly due to the increased viscosity of dispersion and the physical barrier action of graphene to cell coalescence.[19] For all PEI/graphene nanocomposite foams, the cell size distributions were uniform.

The distribution of graphene in cell structure was investigated by SEM micrograph, and the results are shown in Figure 3. At graphene loading of 1 wt %, the cell wall of PEI/graphene nanocomposite foam seemed smooth at lower SEM magnification, and a few graphene sheets were observed on the conjunction of cells at higher SEM magnification. At graphene loading of 7 wt %, the cell structure of PEI/graphene nanocomposite foam was porous, and lots of voids were present among cells, as indicated in SEM micrograph with lower magnification. SEM micrograph with higher magnification verified that these voids were not only composed of the cell structure but also composed of the gaps generated between

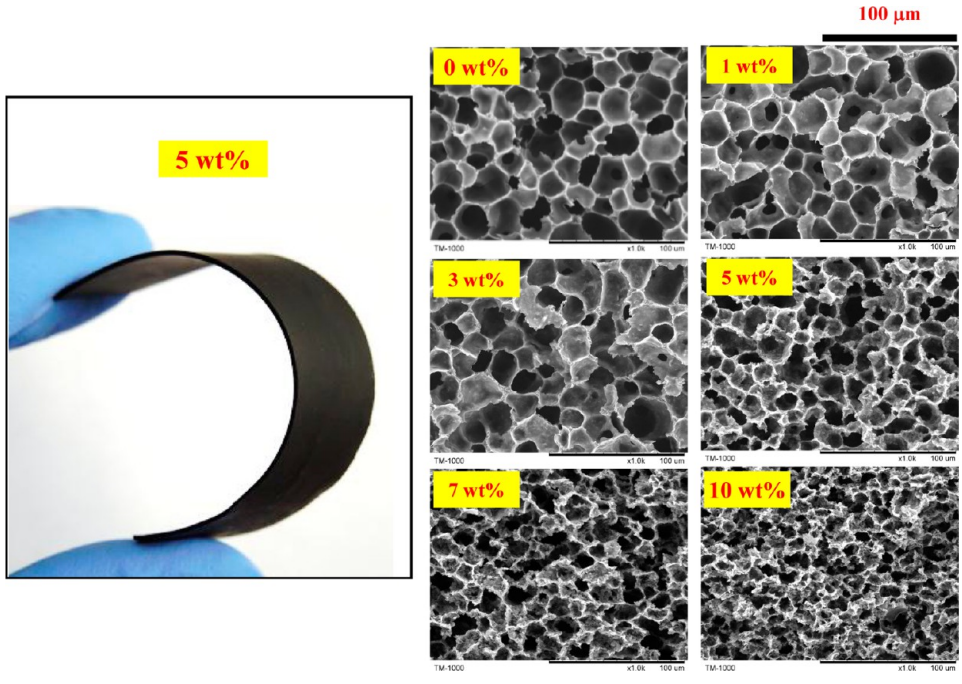

Figure 2. Optical and SEM micrographs of PEI/graphene nanocomposite foams as the function of graphene content.

Table 2. Average Cell Diameter of PEI/Graphene Nanocomposite Foams as the Function of Graphene Content

graphene content (wt %)	0	0.1	0.3	0.5	1	3	5	7	10
average cell diameter (μm)	15.3	15.9	15.9	16.3	16.6	16.1	13.5	12.1	9.0
error bar	±4.5	±4.8	±3.8	±5.1	±4.9	±4.4	±2.5	±1.8	±2.0

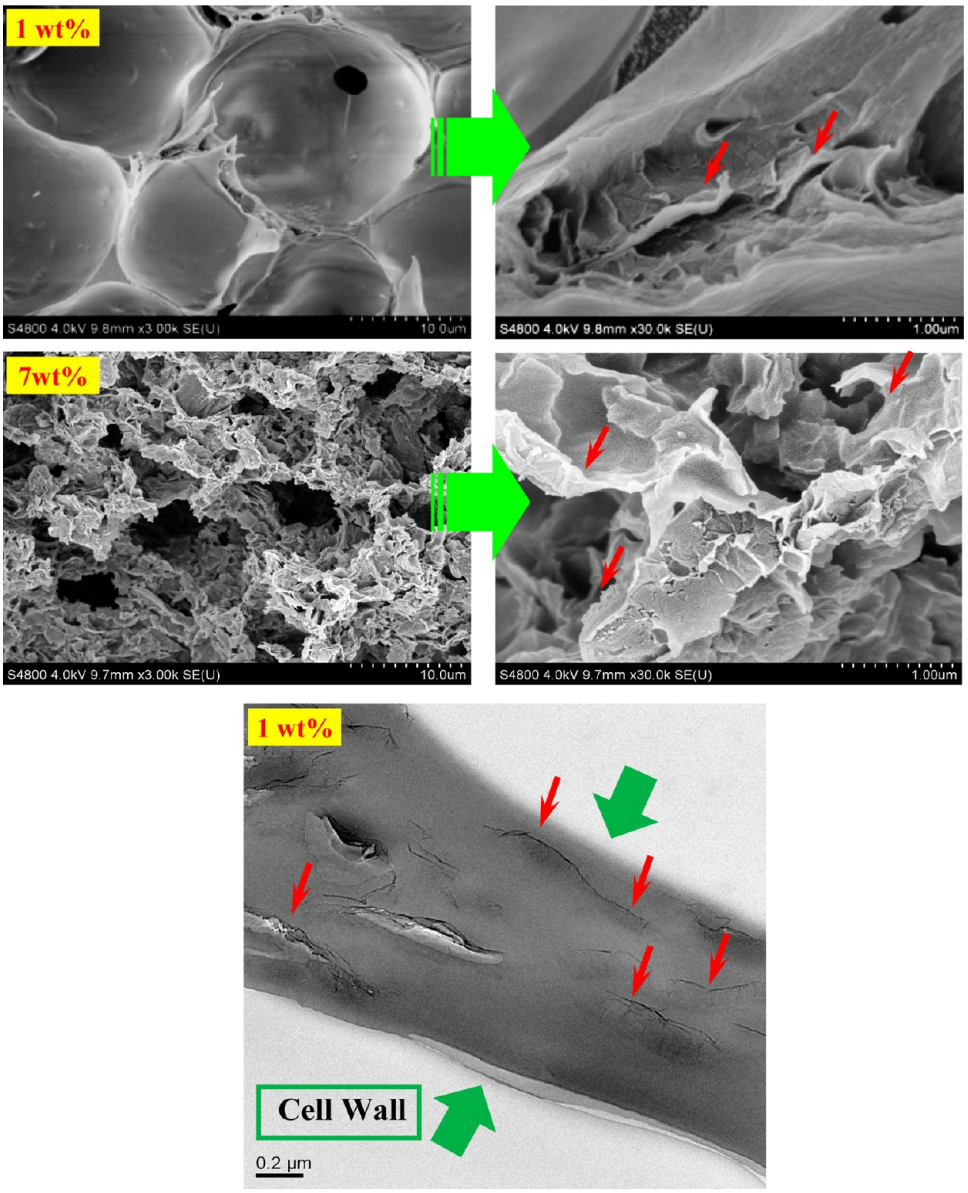

Figure 3. SEM and TEM micrographs to show the dispersion of graphene in PEI/graphene nanocomposite foams. The obvious orientation of graphene on cell wall was observed at the TEM micrograph.

the matrix and the graphene sheets, which may have resulted from the poor distribution of graphene sheets in PEI matrix.

The influence of the foaming process on the dispersion of graphene was explored. It is well accepted that the cell growth process is an extensional flow of polymer solution in nature.[21,22] Our previous study verified that the in situ formed strain rate during cell growth was extremely high, i.e., 20−130 s^{-1}.[23] Since PEI matrix had good interfacial bonding with graphene nanosheets, the applied biaxial stretching action during cell growth was expected to transfer from matrix onto graphene. As indicated in Figure 1, one action of this strong stretching was to push the surrounded graphene and facilitated the enrichment of graphene nanosheets on the cell wall. Furthermore, as indicated by the TEM micrograph in Figure 3, another effect of the strong stretching was to induce the orientation of graphene nanosheets along cell wall.

3.2. EMI Shielding of Microcellular PEI/Graphene Nanocomposite Foams. Electrical conductivity is critical for EMI shielding efficiency, because it is an intrinsic ability of a material for absorbing electromagnetic radiation.[24] The influence of microcellular cell structure on the electrical conductivity of PEI/graphene nanocomposites was investigated, and the results are shown in Figure 4. PEI is a kind of electronic packaging material due to its low electrical conductivity, i.e., 1.2×10^{-19} S/cm in this study. The addition of graphene dramatically increased the volume electrical

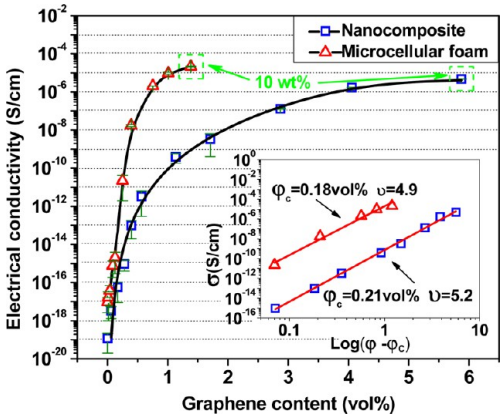

Figure 4. Electrical conductivity for PEI/graphene nanocomposites and microcellular foams as the function of graphene content.

conductivity of the compressed PEI/graphene nanocomposites up to 3.9×10^{-10} S/cm with a 1.13 vol % loading, indicating the formation of conductive percolating network among graphene nanosheets. Compared to PEI/graphene nanocomposite, microcellular PEI/graphene foam possessed a higher electrical conductivity of 1.75×10^{-8} S/cm with a lower graphene loading of 0.39 vol % loading, which suggested that the presence of microcellular structure might decrease the percolation threshold of the conductive composites.

The actual critical graphene concentration was calculated according to the percolation theory:[25]

$$\sigma \propto (\varphi - \varphi_c)^{\upsilon}$$

where σ is the conductivity of the composite, φ is the volume fraction of the graphene, φ_c is the critical volume fraction, and υ is the fitted constant. To obtain the critical volume concentration, the volume conductivity data of PEI/graphene nanocomposites and microcellular foams was fitted to the power law in terms of graphene volume fraction. An excellent fit was achieved between the experimental conductive value and the fit function, with a correlation factor of R = 99% and R = 98% for nanocomposites and microcellular foams, respectively, and the linear relationship was also plotted in the inset of Figure 4. According to the fitting result, the φ_c of PEI/graphene nanocomposite and microcellular foams was 0.21 and 0.18 vol %, respectively.

In general, the foaming process presents two effects on the electrical conductivity percolation threshold of polymer nanocomposite. One effect is that the excluded volume related to cell formation pushes nanoparticles together; even more important, the in situ generated strong extensional flow during bubble growth facilitates the orientation of nanoparticles in cell wall.[23] The enriching and orientation of nanoparticles causes the close pack of nanoparticles in the foamed composites. The other effect of the foaming process is the volume expansion, which tends to increase the distance of adjacent nanoparticles.

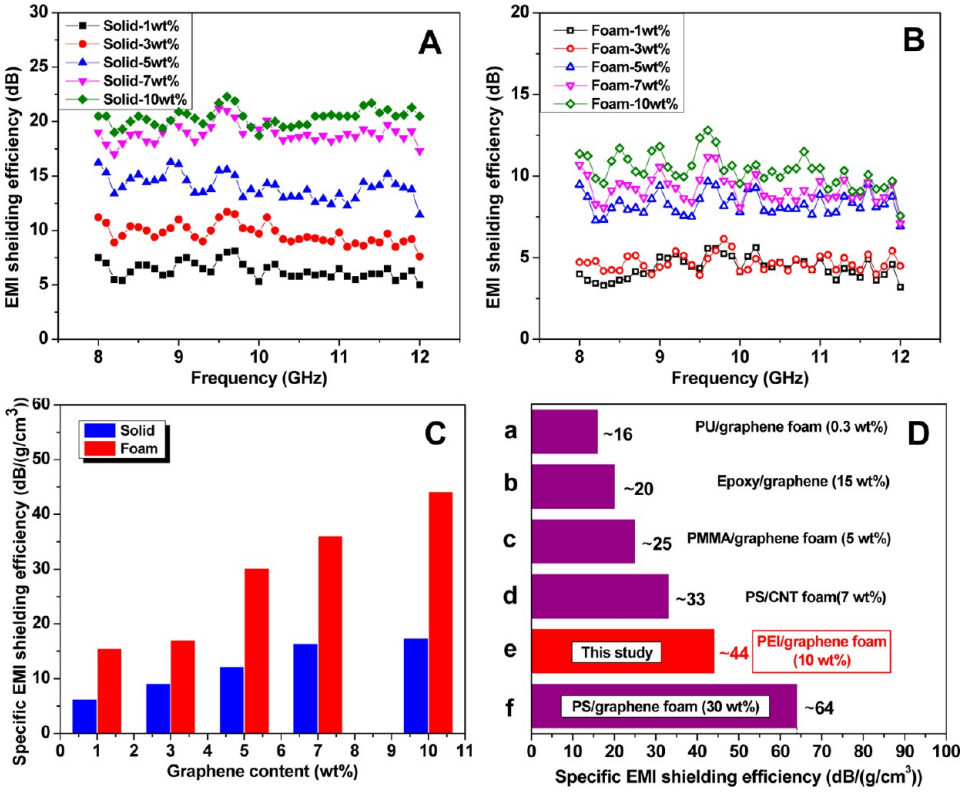

a: obtained from Ref. [14] b: obtained from Ref. [5] c: obtained from Ref. [6] d: obtained from Ref. [9]
e: in this study f: obtained from Ref. [11]

Figure 5. EMI shielding efficiency of (A) PEI/graphene nanocomposite and (B) microcellular foams at different frequency. The specific EMI shielding efficiency of PEI/graphene nanocomposite and microcellular foams at 9.6 GHz (C). The comparative of specific EMI shielding efficiency of our data with other reported results (D). a: obtained from ref 28; b: obtained from ref 5; c: obtained from ref 6; d: obtained from ref 9; e: in this study; f: obtained from ref 11.

Therefore, the electrical conductivity percolation threshold of polymer foam will be determined by the degree of volume expansion. In the study of broad-band electrical conductivity of carbon nanofiber (CNF) reinforced PP foam, Antunes et al. verified that the foaming process decreased the critical CNF concentration for conduction from 6 vol % for solid to 5 vol % for foam, where the volume expansion of PP foam was about 3 times.[26] Another study on PS/graphene foaming reported that the foaming process reduced the electrical conductivity percolation threshold of PS/graphene nanocomposite slightly.[6] Our results demonstrated that the foaming process contributed to a decrease in electrical conductivity percolation threshold from 0.21 to 0.18 vol %, and the volume expansion of foam was about 4 times. We believed that the interesting phenomenon was caused by the enrichment and orientation of graphene during cell growth.

A further increase in graphene loading gradually increased the electrical conductivity of PEI/graphene nanocomposites up to 4.8×10^{-6} S/cm at graphene loading of 5.87 vol %. In the case of PEI/graphene nanocomposite foams, however, we observed a rapid increase in electrical conductivity up to 2.2×10^{-5} S/cm with the graphene loading of 1.38 vol %. It should be pointed out that PEI/graphene nanocomposite (5.87 vol %) and microcellular foams (1.38 vol %) possessed the same graphene loading in weight percentage of 10 wt %, which indicated that the microcellular foaming process was a benefit to the improvement of electrical conductivity of PEI/graphene nanocomposites.

The remarkable enhancement of electrical conductivity potentially endows lightweight PEI/graphene nanocomposite foam with good electromagnetic interference (EMI) shielding property. In this study, the EMI shielding of PEI/graphene nanocomposite and microcellular foams at the X-band (8−12 GHz) was measured. It is seen from Figure 5A,B that the EMI SE of PEI/graphene nanocomposite and microcellular foams exhibited weak frequency dependency at the X-band. The EMI SE of PEI/graphene composites increased gradually up to ∼20 dB at 10 wt % graphene loading. After the volume expansion by 4 times, however, the EMI SE of PEI/graphene nanocomposite foams decreased obviously, and the value of the microcellular foam with 10 wt % graphene loading was about 11 dB. Our results indicated that PEI/graphene nanocomposite foam with 10 wt % graphene addition exhibited a slightly increased electrical conductivity compared to the unfoamed counterpart. The reason for the difference in EMI SE between the two samples was mainly due to the obvious decrease in actual thickness of microwave radiative transfer in the foamed sample. Specifically, for the foam with thickness of 2.3 mm, the compacted thickness without any bubbles was only about 0.54 mm. Therefore, the significant reduction of sample thickness would inevitably decrease the EMI SE of PEI/graphene nanocomposite foam.[27]

The specific EMI shielding efficiency was calculated on the basis of the rate of total EMI shielding efficiency and the sample density, and the results are shown in Figure 5C. Owing to the much lower density of the foamed sheets, the specific EMI shielding efficiency, which represents the material utilizing efficient, would be higher than the solid sheets. The specific EMI SE of microcellular PEI/graphene foams was 36.1 dB/(g/cm^3) for 7 wt % loading and 44.1 dB/(g/cm^3) for 10 wt % loading, which was about 2.2 and 2.5 times higher than the unfoamed counterparts. These results demonstrated that the foaming process dramatically improved the specific EMI SE of PEI/graphene composites. Figure 5D summarizes the specific EMI SE of polymer nanocomposite foams reported by other researchers.[5,6,9,11,29] It seemed that PEI/graphene foam presented a little bit higher specific EMI SE than other foaming systems at similar graphene loading, possibly resulting from the formation of oriented graphene dispersion in cell walls. Yan et al. obtained a much higher specific EMI SE in PS/graphene nanocomposite foam than that reported in this work because of a higher graphene loading of 30 wt %.[11]

The EMI SE of material includes the contribution of SE_R, SE_A, and SE_M. SE_M can be negligible when $SE_A \geq 15$ dB because SE_M is a positive or negative correction term.[29] Though for foamed nanocomposite sheets the shielding value was below 15 dB, we still omitted the multiple internal reflections considering the parallel comparison. Figure 6 summarizes the contribution of SE_A and SE_R. It is seen that the SE_A of PEI/graphene nanocomposites was 7.27−19.66 dB at graphene loading of 3−10 wt %, indicating about 76.2−90.8% electromagnetic energy was absorbed by the materials. The introduction of microcellular structure was verified to further increase the contribution of SE_A to SE_{total}, where about 90.6−98.9% electromagnetic energy was absorbed by the microcellular foams, suggesting the obvious increased absorbing ability of samples with the presence of microcellular structure.

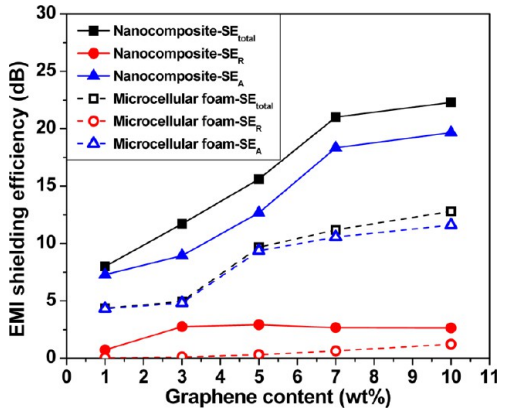

Figure 6. SE_{total}, SE_R, and SE_A of PEI/graphene nanocomposite and microcellular foams at 9.6 GHz.

It is well accepted that the microwave reflection is the result of dielectric mismatch at interfaces. In order to fabricate material with excellent absorption property, the dielectric constant of material must be controlled as close as possible to that of air, i.e., 1.[13] The introduction of tiny air bubbles in polymer matrix by microcellular foaming technology would decrease the dielectric constant without any effect on the component of the matrix.[30] In addition, as indicated in Figure 7, the spherical microscale air bubbles in the foams could attenuate the incident electromagnetic microwaves by reflecting and scattering between the cell wall and nanofillers, and the microwaves were difficult to escape from the sample before being absorbed and transferred to heat.[31] This novel idea to decrease the reflection of microwaves makes polymer nanocomposite foam an excellent microwave absorber compared with the bulk shielding composite. As a consequence, the microcellular foaming method would be an effective choice to enhance the absorption property of the EMI shielding materials.

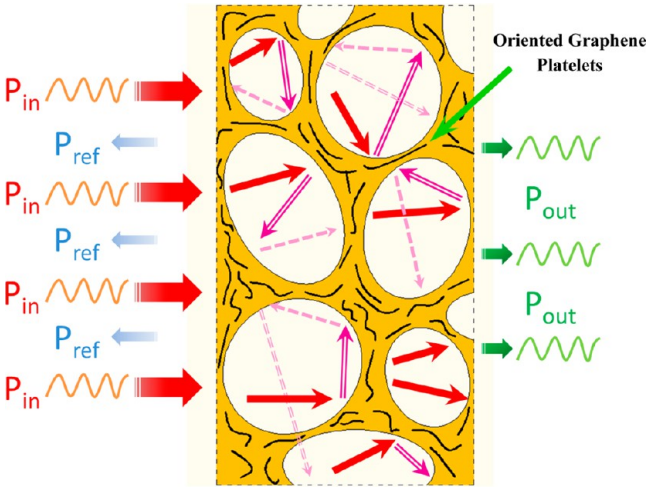

Figure 7. Schematic description of the microwave transfer across PEI/graphene nanocomposite foam.

3.3. Thermal and Tensile Properties of PEI/Graphene Nanocomposite Foam. One of the most attractive properties of polymeric foam is the thermal insulation. As a kind of high performance polymer, PEI can be used at both high and low temperature. Figure 8 summarizes the thermal conductivity of

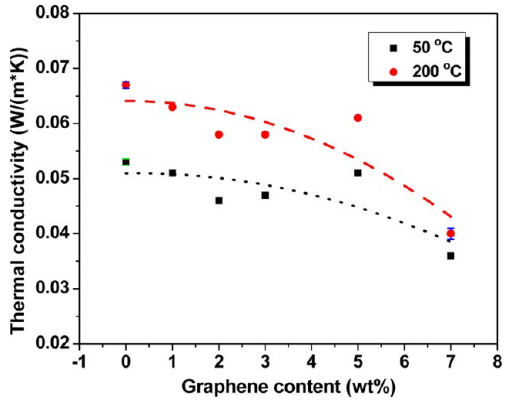

Figure 8. Thermal conductivity of PEI/graphene nanocomposite foams at 50 and 200 °C.

PEI/graphene nanocomposite foams measured at 50 and 200 °C, respectively. PEI foams had a thermal conductivity of 0.053 and 0.067 W/(m·K) at 50 and 200 °C, respectively. With the introduction of graphene, the thermal conductivity of PEI/graphene nanocomposite foams tended to decrease gradually to 0.036 W/(m·K) at 50 °C and 0.040 W/(m·K) at 200 °C for microcellular foam with graphene loading of 7 wt %. This result is very interesting because graphene is one kind of thermal conductive filler, and the addition of graphene was supposed to increase the thermal conductivity of polymer/graphene nanocomposites.[32,33]

In general, several important parameters, i.e., gas conductivity, matrix conductivity, thermal radiation, and convective heat transfer, determine the thermal conductivity of polymeric foams. Since the cell size of the prepared PEI microcellular foam was in the range of microscale, the contribution of the convective heat transfer could be neglected.[34] In this study, the addition of graphene was found to decrease the cell size of PEI/graphene nanocomposite foams, and the decrease in cell size might contribute to the decrease in thermal conductivity of microcellular foams with the same density.[35,36] Carbon particles have been verified to strongly absorb and reflect the infrared (IR) radiation, which depresses the thermal radiation of materials. In the study of polystyrene/carbon particle foaming, Zhang et al. proved that the strong absorption and reflection of IR radiation of carbon particles was the main reason for the decrease in thermal conductivity of polystyrene/carbon foams relative to pure polystyrene foam.[37] Considering graphene possessed much higher specific surface area than that of carbon particle, it might be safe to conclude that graphene presented much higher ability to absorb and reflect the IR radiation. However, regarding the result, further study is needed to fully understand the mechanism behind the phenomenon.

Figure 9 shows the tensile properties of PEI/graphene nanocomposite foams. The tensile strength of pure PEI foam

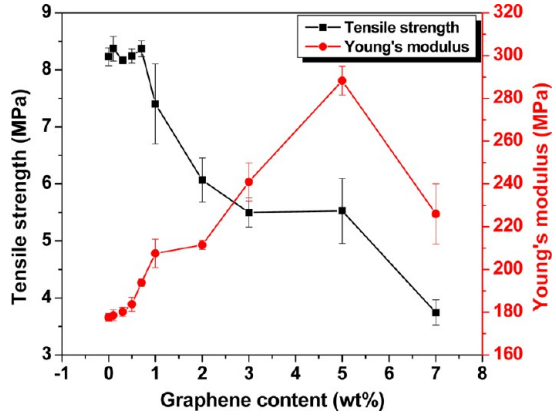

Figure 9. Tensile properties of PEI/graphene nanocomposite foams as a function of graphene content.

was 8.23 MPa. The addition of graphene with content less than 0.7 wt % did not change this value. With the increase in graphene loading, the tensile strength of PEI/graphene nanocomposite foam decreased dramatically to 3.5 MPa at 7 wt %. The introduction of graphene was found to increase the Young's modulus of microcellular PEI foam from ~180 MPa for pure PEI foam to 290 MPa for PEI/graphene foam with graphene loading of 5 wt %. A further increase in graphene content decreased the Young's modulus to 226 MPa at graphene loading of 7 wt %.

4. CONCLUSION

In summary, we have developed a facile and fast approach for scalable fabrication of lightweight PEI/graphene nanocomposite foam with high graphene loading based on a WVIPS process. The in situ generated extensional flow caused the redispersion and orientation of graphene nanosheets on cell wall, which decreased the electrical percolation and increased the specific EMI SE of graphene. Furthermore, PEI/graphene nanocomposite foams exhibited the well-defined thermal insulation and tensile properties. The comprehensive study of PEI nanocomposite foams based on other powerful absorbers will be reported in the future in order to develop the useful materials for EMI shielding in high-tech fields.

AUTHOR INFORMATION

Corresponding Author

*Tel.: +86 0574 8668 5256. Fax: +86 0574 8668 5186. E-mail: wtzhai@nimte.ac.cn.

Notes

The authors declare no competing financial interest.

ACKNOWLEDGMENTS

The authors are grateful to Nanjing Yuezi Chemical Ltd, the National Natural Science Foundation of China (Grant 51003115), and Ningbo Natural Science Foundation (Grant No. 2011A6101118) for their financial support of this study.

REFERENCES

(1) Chung, D. D. L. *Carbon* **2001**, *39*, 279−285.
(2) Chung, D. D. L. *Carbon* **2012**, *50*, 3342−3353.
(3) Geetha, S.; Kumar, K. K. S.; Rao, C. R. K.; Vijayan, M.; Trivedi, D. C. *J. Appl. Polym. Sci.* **2009**, *112*, 2073−2086.
(4) Geim, A. K.; Novoselov, K. S. *Nat. Mater.* **2007**, *6*, 183−191.
(5) Liang, J.; Wang, Y.; Huang, Y.; Ma, Y.; Liu, Z.; Cai, F.; Zhang, C.; Gao, H.; Chen, Y. *Carbon* **2009**, *47*, 922−925.
(6) Zhang, H. B.; Yan, Q.; Zheng, W. G.; He, Z.; Yu, Z. Z. *ACS Appl. Mater. Interfaces* **2011**, *3*, 918−924.
(7) Eswaraiah, V.; Sankaranarayanan, V.; Ramaprabhu, S. *Macromol. Mater. Eng.* **2011**, *296*, 894−898.
(8) Yang, Y. L.; Gupta, M. C.; Dudley, K. L.; Lawrence, R. W. *Adv. Mater.* **2005**, *17*, 1999−2003.
(9) Yang, Y. L.; Gupta, M. C. *Nano Lett.* **2005**, *5*, 2131−2134.
(10) Thomassin, J. M.; Vuluga, D.; Alexandre, M.; Jerome, C.; Molenberg, I.; Huynen, I.; Detrembleur, C. *Polymer* **2012**, *53*, 169−174.
(11) Yan, D. X.; Ren, P. G.; Pang, H.; Fu, Q.; Yang, M. B.; Li, Z. M. *J. Mater. Chem.* **2012**, *22*, 18772−18774.
(12) Zhu, J. H.; Wei, S. Y.; Haldolaarachchige, N.; Young, D. P.; Guo, Z. H. *J. Phy. Chem. C* **2011**, *115*, 15304−15310.
(13) Thomassin, J. M.; Pagnoulle, C.; Bednarz, L.; Huynen, I.; Jerome, R.; Detrembleur, C. *J. Mater. Chem.* **2008**, *18*, 792−796.
(14) Zhai, W. T.; Feng, W. W.; Ling, J. Q.; Zheng, W. G. *Ind. Eng .Chem. Res.* **2012**, *51*, 12827−12834.
(15) Miller, D.; Chatchaisucha, P.; Kumar, V. *Polymer* **2009**, *50*, 5576−5584.
(16) Miller, D.; Kumar, V. *Polymer* **2011**, *52*, 2910−2919.
(17) Zhai, W. T.; Yu, J.; Wu, L. C.; Ma, W. M.; He, J. S. *Polymer* **2006**, *47*, 7580−7589.
(18) Yavari, F.; Rafiee, M. A.; Rafiee, J.; Yu, Z. Z.; Koratkar, N. *ACS Appl. Mater. Interfaces* **2010**, *2*, 2738−2743.
(19) Park, H. C.; Kim, Y. P.; Kim, H. Y.; Kang, Y. S. *J. Membr. Sci.* **1999**, *156*, 169−178.
(20) Elodie, L. *Songklanakarin J. Sci. Technol.* **2002**, *24*, 871−877.
(21) Zhai, W. T.; Kuboki, T.; Wang, L.; Park, C. B.; Lee, E. K.; Naguib, H. *Ind. Eng. Chem. Res.* **2010**, *49*, 9834−9845.
(22) Zhai, W. T.; Park, C. B.; Kontopoulou, M. *Ind. Eng. Chem. Res.* **2011**, *50*, 7282−7289.
(23) Zhai, W. T.; Wang, J.; Chen, N.; Park, C. B.; Naguib, H. *Poly. Eng. Sci.* **2012**, *52*, 2078−2089.
(24) Gelves, G. A.; Al-Saleh, M. H.; Sundararaj, U. *J. Mater. Chem.* **2011**, *21*, 829−836.
(25) Stankovich, S.; Dikin, D. A.; Dommett, G. H. B.; Kohlhaas, K. M.; Zimney, E. J.; Stach, E. A.; Piner, R. D.; Nguyen, S. T.; Ruoff, R. S. *Nature* **2006**, *442*, 282−286.
(26) Antunes, M.; Mudarra, M.; Velasco, J. I. *Carbon* **2011**, *49*, 708−717.
(27) Wang, L. L.; Tay, B. K.; See, K. Y.; Sun, Z.; Tan, L. K.; Lua, D. *Carbon* **2009**, *47*, 1905−1910.
(28) Mar Benal, M.; Molenberg, I.; Estravis, S.; Angel Rodriguez-Perez, M.; Huynen, I.; Angel Lopez-Manchadu, M.; Verdejo, R. *J. Mater. Sci.* **2012**, *47*, 5673−5679.
(29) Al-Saleh, M. H.; Sundararaj, U. *Carbon* **2009**, *47*, 1738−1746.
(30) Krause, B.; Koops, G. H.; van der Vegt, N. F. A.; Wessling, M.; Wubbenhorst, M.; van Turnhout, J. *Adv. Mater.* **2002**, *14*, 1041−1046.
(31) Wang, J. C.; Xiang, C. S.; Liu, Q.; Pan, Y. B.; Guo, J. K. *Adv. Funct. Mater.* **2008**, *18*, 2995−3002.
(32) Planes, E.; Duchet, J.; Maazouz, A.; Gerard, J. F. *Polym. Eng. Sci.* **2008**, *48*, 723−731.
(33) Ghose, S.; Working, D. C.; Connell, J. W.; Smith, J. G.; Watson, K. A.; Delozier, D. M.; Sun, Y. P.; Lin, Y. *High Perform. Polym.* **2006**, *18*, 961−977.
(34) Suh, K. W. Polystyrene and structural foam. In *Handbook of polymeric foams and foam technology*; Klempner, D., Sendijarevic, V., Eds.; Hanser Publisher: Munich, 2004; p 189.
(35) Almanza, O. A.; Rodriguez-Perez, M. A.; De Saja, J. A. *J. Polym. Sci. Polym. Phys.* **2000**, *38*, 993−1004.
(36) Almanza, O.; Rodriguez-Perez, M. A.; de Saja, J. A. *Polym. Int.* **2004**, *53*, 2038−2044.
(37) Zhang, C. L.; Zhu, B.; Lee, L. J. *Polymer* **2011**, *52*, 1847−1855.